RAPID COMMUNICATIONS

PHYSICAL REVIEW B VOLUME 46, NUMBER 17 1 NOVEMBER 1992-I

Particle translational motion and reverse coarsening phenomena in multiparticle systems induced by a long-range elastic interaction

Yunzhi Wang
Department of Materials Science and Engineering, Rutgers University, Piscataway, New Jersey 08855-0909

Long-Qing Chen
Department of Materials Science and Engineering, Penn State University, University Park, Pennsylvania 16802

A. G. Khachaturyan
Department of Materials Science and Engineering, Rutgers University, Piscataway, New Jersey 08855-0909
(Received 5 June 1992)

The kinetics of multiparticle coarsening controlled by a long-range elastic interaction is considered. Without any *a priori* assumptions concerning the morphology of coarsening particles, it is shown that translational motion and reverse coarsening are two important mechanisms responsible for the morphological evolution of initially randomly distributed new phase particles into a regular array in an elastically anisotropic crystal. The general characteristic of the strain-induced coarsening in a multiparticle system is determined by the tendency to form a pseudoperiodical precipitate macrolattice which minimizes the elastic strain energy. It is consistent with previous thermodynamic analyses for two-phase systems with a strong long-range elastic interaction.

The classic Liftshitz-Slyozov-Wagner (LSW) theory[1] describes the microstructure instability driven by reduction in interfacial energy, a phenomenon known as Ostward ripening. This is equivalent to assuming that there are only short-range chemical interactions in the system and hence, the only morphology-dependent part of total free energy is the interfacial energy. However, phase transformations in crystalline solids usually involve crystal lattice rearrangements which result in crystal lattice mismatch between the precipitate and matrix phases. This mismatch is accommodated by elastic displacements which generate strain fields within both phases. Overlap of these strain fields yields a strain-induced interaction whose nature is very different from the chemical interactions. It is long range (decaying as $1/r^3$, where r is the distance between two interacting particles) and in many aspects is similar to the dipole-dipole–type interactions in ferromagnetic or ferroelectric materials. Consequently the elastic strain energy, unlike the interfacial energy, depends on both the volume and morphology of the two phases. It makes the bulk free energy a driving force for morphological transformations. Under such a circumstance, the coarsening behaviors should be dramatically different from the Ostward ripening and could not be described by the LSW theory.

The transformation-induced elastic strain effect on microstructural evolutions has long been recognized.[2,3] A subject of particular interest recently is the strain-induced coarsening in two-phase coherent solids. Some intriguing phenomena such as strong directional alignments and spatial correlations of precipitates,[4–7] particle shape transition including splitting,[8–11] suppression, and reversion of coarsening[12–15] were observed and predicted. Due to complexity of the analyzed systems, however, theoretical treatments to date deal with only a limited number of simplified configurations and most of them are based on thermodynamic arguments. Coarsening kinetics of two spherical particles which takes into account the coherency strain effect in an elastically anisotropic system was recently investigated by Johnson, Abinandanan, and Voorhees.[16] They obtained a diffusional drift of the two particles towards each other if they are aligned along the elastically soft direction, accompanied by a reverse coarsening when their relative size falls into certain range (the latter effect was previously predicted in Ref. 14).

In this paper we try to formulate the problem in more general terms which relax all constraints on the number of particles, particle morphology and its evolution path, and the diffusion fields around and inside the particles which were imposed in the earlier works.[4,6–8,14–16] More specifically, we introduce arbitrary number of particles with arbitrary distributions. The particles are free to change their shapes in accordance with the interplay between the morphological dependent energies during coarsening. Atomic diffusion is allowed within both phases as well as along the interfaces. No special interfacial boundary conditions are assumed. The diffusion field and concentration profiles in the system automatically follow from the computer simulation. Within this approach, the dynamics of coarsening resulting in the pseudoperiodical arrangement of precipitates from initially randomly distributed new phase particles in an elastically anisotropic system is investigated. It will be shown that particle translational motion and reverse coarsening are two major underlying mechanisms.

To describe an arbitrary two-phase morphology, it is convenient to introduce the single-site occupation probability function, $n(\mathbf{r},t)$, of finding a solute atom at the crystal lattice site $\mathbf{r}$ and at time t. We start from an initial state consisting of small equiaxed (introduction of the equiaxed shape is not necessary but for convenience and for the reason that particles usually have equiaxed shapes when they are very small) particles (nuclei) of the precipitate phase randomly distributed in a parent phase matrix.

It is described by the function $n(\mathbf{r},0)$ which is equal to $c_{\alpha'}$ if a point $\mathbf{r}$ is within a particle and c_0 otherwise, where $c_{\alpha'}$ and c_0 are compositions of the equilibrium precipitate phase α' and the initial matrix. Growth and coarsening of the small particles in a combined concentration and strain field are then described by the relaxation of the function $n(\mathbf{r},t)$ with time, t, through the nonlinear microscopic diffusion equation[17]

$$\frac{dn(\mathbf{r},t)}{dt}=\sum_{\mathbf{r}'}L_0(\mathbf{r}-\mathbf{r}')\frac{\delta F}{\delta n(\mathbf{r}',t)}\ , \tag{1}$$

where $L_0(\mathbf{r}-\mathbf{r}')$ is a matrix of kinetic coefficients characterizing the probability of an elementary diffusional jump from site $\mathbf{r}$ to $\mathbf{r}'$ during a time unit and F is the total free energy which includes the elastic strain energy. The variational derivative, $\delta F/\delta n(\mathbf{r}',t)$, forms the total thermodynamic driving force for the relaxation of $n(\mathbf{r},t)$. Equation (1) allows us to exclude assumptions concerning the boundary conditions between coexisting phases and the fixed spherical shapes, which were usually imposed by the traditional treatments.[16] The nonlinearity of the equation automatically "takes care" of all the problems.

Since the focus of the present paper is the strain-induced coarsening of a multiparticle system, any free-energy approximation which provides a convex segment on the free energy versus composition curve corresponding to a miscibility gap would result in the same morphological transformation sequence. We use the simplest one, the mean-field free energy

$$F=\frac{1}{2}\sum_{\mathbf{r},\mathbf{r}'}W(\mathbf{r}-\mathbf{r}')n(\mathbf{r})n(\mathbf{r}')$$
$$+k_BT\sum_{\mathbf{r}}\{n(\mathbf{r})\ln n(\mathbf{r})+[1-n(\mathbf{r})]\ln[1-n(\mathbf{r})]\} \tag{2}$$

where $W(\mathbf{r}-\mathbf{r}')=w(\mathbf{r}-\mathbf{r}')_f+w(\mathbf{r}-\mathbf{r}')_{\rm el}$ is a pairwise interaction energy between atoms at lattice sites $\mathbf{r}$ and $\mathbf{r}'$, including the short-range chemical interaction $w(\mathbf{r}-\mathbf{r}')_f$ and the long-range strain-induced interaction $w(\mathbf{r}-\mathbf{r}')_{\rm el}$ (introduction of the long-range elastic interaction and consideration of low temperatures make the mean-field model reasonably accurate[18]) and k_B is the Boltzmann constant. The bulk free energy, interfacial energy, and strain energy defined in conventional thermodynamics are automatically described by Eq. (2). Its long-wave limit transition yields the Cahn-Hilliard equation.[3]

The nonlinear diffusion equation (1) was solved numerically in the reciprocal space. For the sake of computational simplicity, a two-dimensional (2D) model system is considered. It is a prototype binary substitutional solid solution with a square lattice. The computational supercell consists of 128×128 unit cells and periodic boundary conditions are applied along both dimensions.

The solid solution is a disordered phase at high temperatures and a two-phase mixture of a solute-lean disordered phase α and a solute-rich disordered phase α' at low temperatures. The short-range chemical interaction is considered up to the second nearest neighbors and the ratio of the pairwise interchange energies of the first and second neighbors is chosen to be $\sqrt{2}$ which provides equal interfacial energies of $\{10\}$ and $\{11\}$ interfaces. The long-range strain-induced interaction is described by utilizing the microscopic elasticity theory.[3,14] We assume that the two product phases α and α' have the same cubic structure and elastic moduli, but different compositions and thus different crystal lattice parameters. Then the Fourier transform of $w(\mathbf{r})_{\rm el}$ can be well approximated as

$$B(\mathbf{e})\approx B(e_x^2e_y^2-\tfrac{1}{8})\ , \tag{3}$$

where e_x and e_y are components of the unit vector $\mathbf{e}$ along the x and y axes in the reciprocal space and B is a material constant that characterizes the elastic properties and the crystal lattice mismatch. In our simulation, B is expressed in a reduced form which is defined as $B^*=B/|V(0)_f-B/8|$ where $V(0)_f$ is the value of the Fourier transform of $w(\mathbf{r})_f$ at $\mathbf{k}=0$, where $\mathbf{k}$ is the reciprocal lattice vector. $B^*>0$ characterizes systems with a negative elastic anisotropy.

The above interatomic interactions provide decomposition when the system is quenched into low temperatures. The phase diagram, presented in terms of a reduced temperature

$$T^*=\frac{k_BT}{|V(0)_f-B/8|}\ ,$$

is shown in Fig. 1.

The initial morphologies for the computer simulation are shown in Fig. 2(I)(a) and 2(II)(a). Each of them consists of 56 α' phase nuclei randomly placed in a homogeneous disordered matrix. The nuclei are simulated by very small equiaxed particles of different sizes. Their sizes and positions are generated by a random-number generator. Two types of occupation probabilities, $n(\mathbf{r})=c_{\alpha'}$ inside the nuclei and $n(\mathbf{r})=c_0$ outside, are assumed. The value of c_0 is determined by the average alloy composition which is chosen to be 0.14. Because only two types of occupation probabilities are assumed and the sizes of the particles are commensurable with the crystal lattice parameter, the nuclei have different shapes such as square, octagon, *et al.* at the initial stage. The selected aging temperature $T^*=0.12$ is represented by an open circle right above the spinodal line in the phase diagram. Temporal evolutions of the initial microstructures during isothermal aging in two different cases, with and

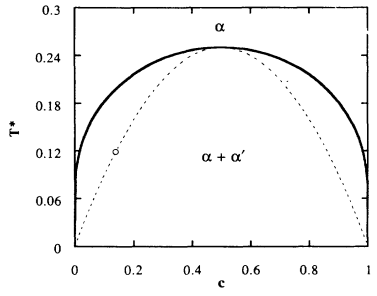

FIG. 1. Coherent equilibrium phase diagram of the model system. The miscibility gap is designated by a solid line and the dashed line describes the spinodal. The diagram is presented in terms of a reduced temperature $T^*=k_BT/|V(0)_f-B/8|$ [see text for the definition of $V(0)_f$ and B]. The open circle represents the alloy composition and "aging" temperature chosen for the computer simulation.

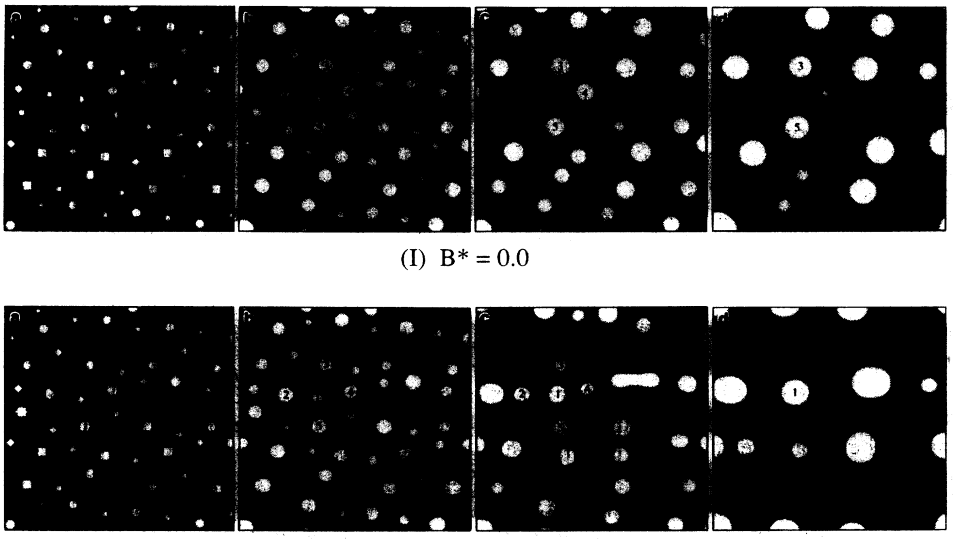

(I) B* = 0.0

(II) B* = 0.35

FIG. 2. Simulated temporal isothermal evolutions of randomly distributed small particles in alloys without ($B^*=0$) and with ($B^*=0.35$) the long-range strain-induced interaction. Various shades of grey represent different values of occupation probability of solute atoms (completely white represents a value of one while completely dark represents a value of zero). (a)–(d) in both (I) and (II) correspond to reduced transformation time $t^*=0$, 200, 1000, and 3000.

without the long-range elastic interaction, are presented in Fig. 2(I)(b)–2(I)(d) and 2(II)(b)–2(II)(d), respectively. They are described by a dimensionless reduced time, $t^*=t/\tau$, where τ is a typical time of the elementary diffusion jumps. Only nearest-neighbor diffusional jumps are allowed in this study. In these figures, completely dark regions in the simulated microstructures represent a zero occupation probability $n(\mathbf{r},t)$ for solute atoms, while completely white regions describe an occupation probability equal to one. All the intermediate values of $n(\mathbf{r},t)$ are represented by different shades of grey.

In the absence of the long-range elastic interaction [Fig. 2(I)], the nuclei grow into circular particles. Coarsening of the circular particles simply follows the LSW mechanism, i.e., large particles grow and smaller ones shrink, leaving the particle shape and mutual arrangement unaltered. These behaviors are clearly demonstrated in Fig. 3(I) where 3(I)(a) is the superimposition of Fig. 2(I)(a) on 2(I)(c) and 3(I)(b) is the superimposition of Fig. 2(I)(a) on 2(I)(d). The small bright spots shown in the pictures represent the initial nuclei and the large light-grey spots describe the coarsening particles at different stages (shades of grey in this figure do not represent real scales of the occupation probability function). From the relative positions of the bright spots with respect to the light-grey ones, we can see that the centers of mass of the coarsening particles are almost unchanged. The slight deviation of some of the bright spots from the centers of the light-grey ones is caused by the interparticle diffusional interactions, which is consistent with the computer simulation by Voorhees *et al.*[19] for the stress-free model.

The strain-induced interaction dramatically changes the coarsening behaviors [see Fig. 2(II)]. First, the nuclei grow into equiaxed particles rather than circular ones and the particles keep changing their shape during coarsening. This shape change is caused by an uphill diffusion driven by the strain-induced variation of the chemical potential along the interface. The solute atoms diffuse from one site (unfavorable) of the interface to another (favorable) to equalize the chemical potential.

Second, a significant particle translational motion (change of center of mass) is observed. It is demonstrated in Fig. 3(II)(a), the superimposition of Fig. 2(II)(a) on 2(II)(c). Comparison of Fig. 3(II)(a) with 3(I)(a) shows that during the strain-induced coarsening the initially randomly distributed particles (bright spots) tend to align themselves along the elastically soft directions. As a result, a regular array which looks like a rough precipitate "macrolattice" is formed [see, e.g., Fig. 2(II)(d)]. This result is consistent with the thermodynamic analysis proposed by Khachaturyan and Airapetyan[6] (according to Ref. 6, if equiaxed new phase precipitates are coherently embedded in a matrix, a minimum energy state is reached when the particles form one of the 14 Bravais lattices).

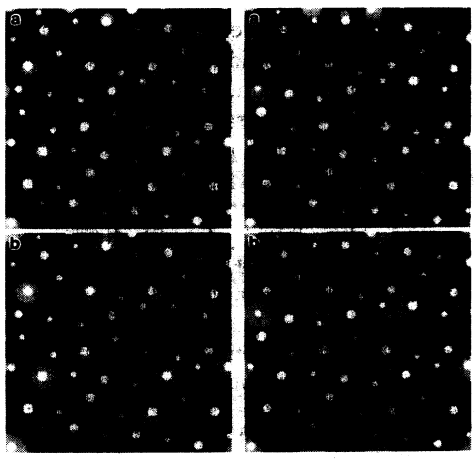

(I) B* = 0.0 (II) B* = 0.35

FIG. 3. Superimpositions of Figs. 2(I)(a) and 2(II)(a) on 2(I)(c) and 2(II)(c) and 2(I)(a) and 2(II)(a) on 2(I)(d) and 2(II)(d) showing unusual behaviors of train-induced coarsening (II) with respect to the Ostward ripening (I). The small bright spots represent initial positions of the particles shown in (a) of Figs. 2(I) and (II) and the large light-grey spots show distributions of the coarsening particles in different stages. Shades of grey in these pictures do not represent real scales of the occupation probability function.

The pseudoperiodical pattern caused by the strain relaxation becomes more pronounced at later stages of coarsening when the surface-to-volume ratio of the particles decreases and thus the contribution of the volume dependent elastic energy increases. The macrolattice "periodicity" is determined by the thermodynamic factor (balance between the strain and interfacial energies) and the diffusion kinetics.

Another unique feature of the strain-induced coarsening could be found if, for example, we concentrate on the coarsening behaviors of the group of particles marked 1, 2, 3, 4, and 5 in Fig. 2(I) and 2(II). The coarsening of those particles shown in Fig. 2(I) where the strain effects are not taken into account follows the conventional Ostward ripening mechanism: large particles grow at the expense of smaller ones. However, if the strain energy is taken into account [see Fig. 2(II)], the initially smaller particle (No. 1) grows larger at the expense of the surrounding larger ones (Nos. 2, 3, 4, and 5). This behavior is just opposite to the Ostward ripening and is called reverse coarsening.

It is interesting that the reverse coarsening and particle translational motion in a multiparticle system predicted here is quite different from that predicted by Khachaturyan and Shatalov[14] and by Johnson, Abinandanan, and Voorhees[16] for a two-particle system. For example, according to Refs. 14 and 16 the reverse coarsening in a two-particle system is characterized by a tendency of the particles to equalize their size driven by an attractive strain-induced interaction when they are aligned along the elastically soft directions. In our simulation, however, the reverse coarsening is directed to provide a pseudoperiodical particle arrangement. As illustrated in Fig. 2(II), the large particles (Nos. 2, 3, 4, and 5) initially located at "interstitial sites" would eventually disappear. As to the particle translational motion, it was predicted in Ref. 16 that the two particles tend to migrate towards each other when they are aligned along the elastically soft direction and away from each other when they are aligned along the elastically hard direction. In a multiparticle system, however, the direction of particle migration is dominated by their locations with respect to the "stable" positions at the "macrolattice sites." Therefore, it is clear from our simulation that the strain-induced coarsening kinetics (e.g., the characters of the particle growth and shrinkage and the directions of the translational motion) is mostly determined by the multiparticle effects and can hardly be interpreted in the framework of the two-particle model.

The kinetics predicted in this paper provide a clue for understanding the formation of strongly correlated precipitate array developed from the initially randomly distributed small particles in Ni-Al (Ref. 4) and Ni-Cu-Si (Ref. 5) alloys. It should be mentioned that in our calculation a homogeneous modulus approximation is used. As has been shown by Voorhees and Johnson for two spherical particle coarsening[20] and by Kawasaki and Enomoto for multiple sphere particle coarsening[21] in elastically isotropic systems, and more recently by Onuki and Nishimori in their 2D computer simulations of spinodal decomposition based on a time-dependent Ginzburg-Landau model,[22] the modulus mismatch between the two phases may also affect the coarsening kinetics.

We gratefully acknowledge support by National Science Foundation Grant No. NSF-DMR-9123167. The simulation was performed on Cray-YMP at the Pittsburgh Supercomputing Center.

[1]I. M. Lifshitz and V. V. Slyozov, J. Phys. Chem. Solid **19**, 35 (1961); C. Wagner, Z. Elektrochem. **65**, 581 (1961).

[2]J. W. Cahn, Acta Metall. **9**, 795 (1961); **10**, 179 (1962).

[3]A. G. Khachaturyan, Fiz. Tverd. Tela (Leningrad) **8**, 2709 (1966) [Sov. Phys. Solid State **8**, 2163 (1967)]; *Theory of Structural Transformations in Solids* (Wiley, New York, 1983).

[4]A. Ardell and R. B. Nicholson, Acta Metall. **14**, 1295 (1966).

[5]Yu. D. Tyapkin, N. T. Travina, and T. V. Yevtsushenko, Phys. Met. Metall. **45** (3), 140 (1978); Yu. D. Tyapkin, I. V. Gongadze, and Ye. I. Maliyenko, Phys. Met. Metall. **66** (3), 160 (1988).

[6]A. G. Khachaturyan and V. M. Airapetyan, Phys. Status Solidi (a) **26**, 61 (1974).

[7]V. Perkovic, C. R. Purdy, and L. M. Brown, Acta Metall. **27**, 1075 (1979).

[8]T. Miyazaki, H. Imamura, and T. Kozakai, Mater. Sci. Eng. **54**, 9 (1982); M. Doi, T. Miyazaki, and T. Wakatsuki, *ibid.* **74**, 139 (1985).

[9]M. J. Kaufman, P. W. Woorhees, W. C. Johnson, and F. S. Biancaniello, Metall. Trans. A **20**, 2171 (1989).

[10]A. G. Khachaturyan, S. V. Semenovskaya, and J. W. Morris, Acta Metall. **36**, 1563 (1988).

[11]Y. Wang, L. Q. Chen, and A. G. Khachaturyan, Scripta Metall. **25**, 1387 (1991); M. MeComack, A. G. Khachaturyan, and J. W. Morris, Jr., Acta Metall. Mater. **40**, 325 (1992).

[12]T. Miyazaki, M. Doi, and T. Kozakai, in *Non Linear Phenomena in Materials Science,* edited by L. P. Kubin and G. Martin, Solid State Phenomena, Vols. 3 and 4 (CNRS, Paris, 1988), p. 227.

[13]R. A. MacKay and M. V. Nathal, Acta Metall. Mater. **38**, 993 (1990).

[14]A. G. Khachaturyan and G. A. Shatalov, Fiz. Tverd. Tela (Leningrad) **11**, 159 (1969) [Sov. Phys. Solid State **11**, 118 (1969)].

[15]W. C. Johnson, Acta Metall. **32**, 465 (1984).

[16]W. C. Johnson, T. A. Abinandanan, and P. W. Voorhees, Acta Metall. **38**, 1349 (1990).

[17]A. G. Khachaturyan, Fiz. Tverd. Tela (Leningrad) **9**, 2594 (1967) [Sov. Phys. Solid State **9**, 2040 (1968)].

[18]R. A. Suris, Fiz. Tverd. Tela (Leningrad) **4**, 1154 (1962) [Sov. Phys. Solid State **4**, 850 (1962)]; V. G. Vaks, A. I. Larkin, and S. A. Pikin, Zh. Eksp. Teor. Fiz. **51**, 240 (1966) [Sov. Phys. JETP **24**, 240 (1967)].

[19]P. W. Voorhees, G. B. McFadden, R. F. Bolsvert, and D. I. Meiron, Acta Metall. **36**, 207 (1988).

[20]P. W. Voorhees and W. C. Johnson, Phys. Rev. Lett. **61**, 2225 (1988); W. C. Johnson, P. W. Voorhees, and D. E. Zupon, Metall. Trans. A **20**, 1175 (1989).

[21]K. Kawasaki and Y. Enomoto, Physica A **150**, 463 (1988).

[22]H. Nishimori and A. Onuki, J. Phys. Soc. Jpn. **60**, 1208 (1991); A. Onuki and H. Nishimori, Phys. Rev. B **43**, 13 649 (1991).

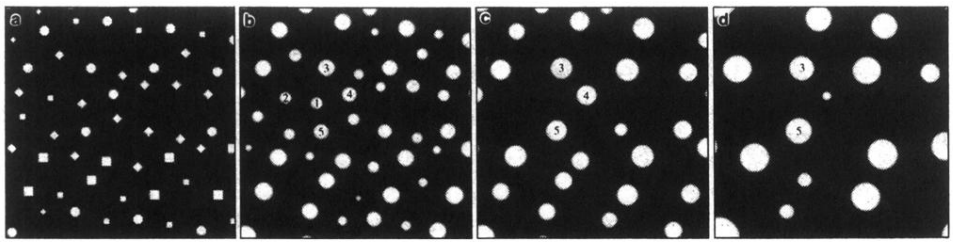

(I) B* = 0.0

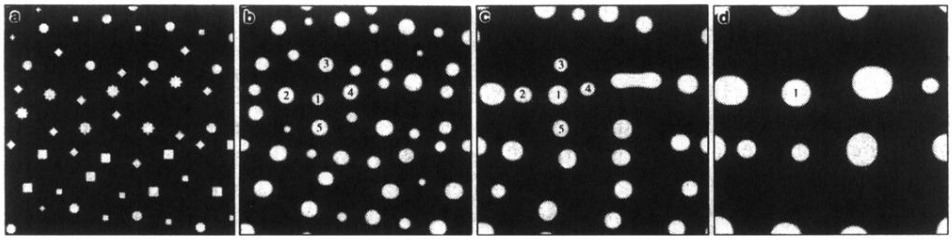

(II) B* = 0.35

FIG. 2. Simulated temporal isothermal evolutions of randomly distributed small particles in alloys without ($B^*=0$) and with ($B^*=0.35$) the long-range strain-induced interaction. Various shades of grey represent different values of occupation probability of solute atoms (completely white represents a value of one while completely dark represents a value of zero). (a)–(d) in both (I) and (II) correspond to reduced transformation time $t^*=0$, 200, 1000, and 3000.

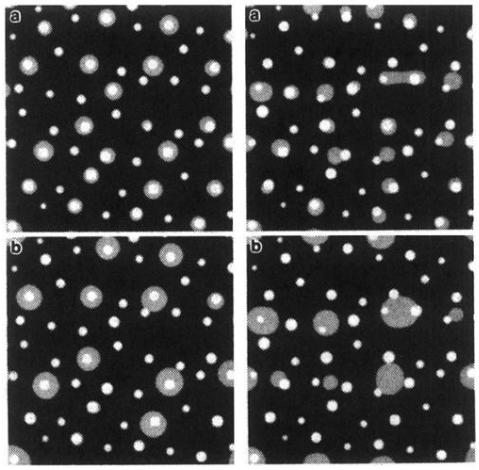

(I) B* = 0.0 (II) B* = 0.35

FIG. 3. Superimpositions of Figs. 2(I)(a) and 2(II)(a) on 2(I)(c) and 2(II)(c) and 2(I)(a) and 2(II)(a) on 2(I)(d) and 2(II)(d) showing unusual behaviors of train-induced coarsening (II) with respect to the Ostward ripening (I). The small bright spots represent initial positions of the particles shown in (a) of Figs. 2(I) and (II) and the large light-grey spots show distributions of the coarsening particles in different stages. Shades of grey in these pictures do not represent real scales of the occupation probability function.